chemistry

MDPI

Article

A Nitrogen-Rich Luminescent Zn(II) Coordination Polymer Based on a 2,4,6-Tris(di-2-pyridylamino)-1,3,5-triazine for Differential Fluorescent Sensing of Antibiotics in Aqueous Medium

Sajeetha Parveen Banu, Mannanthara Kunhumon Noushija, Binduja Mohan and Sankarasekaran Shanmugaraju *

Department of Chemistry, Indian Institute of Technology Palakkad, Kanjikode 678623, Kerala, India; 202205011@smail.iitpkd.ac.in (S.P.B.); 202114001@smail.iitpkd.ac.in (M.K.N.); 201914001@smail.iitpkd.ac.in (B.M.)
* Correspondence: shanmugam@iitpkd.ac.in

Abstract

The design of suitable chemosensors for environmental pollutants and toxins detection at trace levels remains a critical area of research. Among various chemosensors, Zn(II) coordination polymers have garnered special interest as fluorescent probes for environmental applications. In this article, we report the synthesis of a nitrogen-rich luminescent Zn(II) coordination polymer, **TDPAT-Zn-CP**, designed for differential fluorescent sensing of antibiotics in an aqueous medium. **TDPAT-Zn-CP** was synthesized using a star-shaped 2,4,6-tris(di-2-pyridylamino)-1,3,5-triazine (TDPAT) fluorophore, a promising blue-emitting compound. The morphological and structural properties of **TDPAT-Zn-CP** were thoroughly analyzed using conventional spectroscopic and analytical techniques. The fluorescence titration studies in aqueous medium demonstrated that **TDPAT-Zn-CP** exhibits remarkable selectivity, sensitivity, and differential fluorescence sensing responses towards various antibiotics. Among the antibiotics tested, **TDPAT-Zn-CP** displayed a significant fluorescence quenching and high selectivity for sulfamethazine (SMZ), with a Stern–Volmer quenching constant of $K_{SV} = 1.68 \times 10^4$ M^{-1} and an impressive sensitivity of 4.95 ppb. These results highlight the potential of **TDPAT-Zn-CP** as a practically useful, highly effective polymeric sensor for the differential fluorescence-based detection of antibiotics in water, offering a promising approach for environmental monitoring and contamination control.

Keywords: Zn(II) coordination polymer; infinite coordination polymer particles; fluorescence sensors; antibiotics; sulfamethazine

check for updates

Academic Editor: Guoqi Zhang

Received: 25 May 2025
Revised: 7 June 2025
Accepted: 24 June 2025
Published: 25 June 2025

Citation: Banu, S.P.; Noushija, M.K.; Mohan, B.; Shanmugaraju, S. A Nitrogen-Rich Luminescent Zn(II) Coordination Polymer Based on a 2,4,6-Tris(di-2-pyridylamino)-1,3,5-triazine for Differential Fluorescent Sensing of Antibiotics in Aqueous Medium. *Chemistry* **2025**, *7*, 108. https://doi.org/10.3390/chemistry7040108

Copyright: © 2025 by the authors. Licensee MDPI, Basel, Switzerland. This article is an open access article distributed under the terms and conditions of the Creative Commons Attribution (CC BY) license (https://creativecommons.org/licenses/by/4.0/).

1. Introduction

Since the discovery of penicillin, antibiotics have revolutionized human and animal health, offering significant advancements in treating bacterial infections [1,2]. In many regions, veterinary antibiotics are routinely incorporated into animal feeds to promote growth and improve feed efficiency [3]. However, the widespread use of these antibiotics has led to their excretion in urine and feces, often in biologically active forms, which poses a serious environmental risk [4]. Many antibiotics find their way into effluent and sludge from wastewater treatment plants, hospitals, and animal farms, ultimately contaminating surrounding ecosystems, including water bodies and soil [5,6]. The improper disposal of antibiotics has contributed significantly to the growing environmental issue known

as "antibiotic pollution" [7]. The World Health Organization (WHO) has identified antibiotic resistance as a major global threat, with profound implications for public health and the economy [8]. Many antibiotics, including tetracyclines, penicillins, β-lactams, and fluoroquinolones, have been classified as emerging environmental pollutants due to their persistence in the environment and their detrimental impact on living organisms and ecosystems [9]. Long-term antibiotic use can lead to a range of adverse health effects, including impaired immunity, increased susceptibility to allergic reactions, hepatotoxicity, genetic disorders, gastrointestinal issues, and other health complications [10]. As a result, controlling the misuse and improper disposal of antibiotics has become essential in mitigating the risks associated with antibiotic resistance, thereby safeguarding both public health and the environment [11].

In response to these concerns, several countries have established maximum residue limits (MRLs) for antibiotics in food and animal feed, necessitating the use of advanced analytical techniques for accurate detection [12]. Monitoring antibiotics at trace levels and adjusting dosages accordingly are critical to reducing the prevalence of antibiotic-resistant microorganisms [13]. Therefore, developing practical, effective, and highly selective detection methods for identifying and analyzing antibiotics is crucial for preserving human health and preventing the further spread of resistance [12–14]. While techniques such as high-performance liquid chromatography (HPLC), ion mobility spectrometry, electrokinetic capillary chromatography, gas chromatography, and Surface-Enhanced Raman Spectroscopy (SERS) are commonly employed for the identification and detection of antibiotics, their use is often limited by factors such as prolonged processing times, low sensitivity, and high costs [15–17]. These methods also require skilled operators and incur substantial operating expenses, which can hinder their widespread adoption and effectiveness [17,18]. Despite the advancement of chemical treatment methods, including photolysis, hydrolysis, thermolysis, technical oxidation processes, and biodegradation, technologies for the efficient detection and removal of antibiotics remain in the early stages of development [19]. In recent years, there has been a growing focus on developing portable, cost-effective, and reliable technologies for the selective detection and removal of antibiotic contaminants from aquatic environments [20]. Among these, fluorescence-based detection and surface adsorption techniques have emerged as promising solutions due to their simplicity, high sensitivity, and enhanced adsorption efficiency [21,22]. However, the challenge remains in identifying materials that can offer both high selectivity and exceptional sensitivity for detecting specific antibiotics [23,24].

Coordination polymers (CPs) represent a promising class of inorganic–organic hybrid materials, gaining significant attention for their diverse applications in detection, sensing, and adsorption [25–29] owing to their unique electrical and optical properties, large surface areas, and remarkable flexibility. Additionally, miniaturized CPs exhibit size-dependent physicochemical properties, distinguishing them from bulk crystalline forms. The reduction in the particle size of crystalline bulk CPs to the micrometer and nanometer scale allows better dispersion in aqueous phases, improved interaction with target analytes, and enhanced sensing capabilities [30]. Despite their potential, the development of luminous nanoscale CPs for fluorescence-based antibiotic detection remains limited. We have shown recently that the selectivity of CPs can be improved by introducing Lewis basic functional groups, such as pyridines and amines, in the polymer backbone [30,31]. These polar functional groups can interact with the hydrogen bond donor sites present in antibiotics, enhancing the binding affinity and selectivity of CPs for specific antibiotic analytes, thereby offering a more effective and targeted detection strategy.

In general, CPs are synthesized by reacting organic linkers with metal ions in an appropriate molar ratio and suitable solvents [25]. The functional properties of CPs can

be tailored by selecting the right organic linkers. 2,4,6-Tris(di-2-pyridylamino)-1,3,5-triazine (TDPAT) is a star-shaped ligand widely used in the field of coordination chemistry, particularly for the design and synthesis of different kinds of CPs [32]. TDPAT consists of a central triazine ring, with three di-2-pyridylamino (DPA) groups attached to the 2, 4, and 6 positions of the triazine core. The triazine core provided a rigid backbone that imparts structural integrity to the polymer. Each DPA unit contains nitrogen donor atoms that can readily coordinate with metal ions, making TDPAT a multifunctional ligand capable of forming robust coordination polymers with distinct properties, such as high mechanical stability, tunable porosity, and the ability to undergo selective binding. Zn(II) is an ideal candidate for the design of CPs due to its d^{10} electronic configuration, which imparts significant flexibility to the coordination of the resulting complexes [31,32]. This unique property allows the geometry of the complexes to be easily tuned, ranging from tetrahedral to square pyramidal and trigonal bipyramidal configurations, ultimately transitioning to octahedral structures, with varying degrees of distortion. The precise control of these geometries can be achieved by carefully selecting ligands and adjusting the molar ratios. Additionally, the inherent lability of bonds in Zn(II) complexes, coupled with the low zero-field stabilization energy, facilitates reversible coordination bond formation, enabling dynamic ligand rearrangement during polymerization [30,33]. This dynamic process supports the formation of diverse, highly ordered networks, offering great potential for the design of versatile and functional CPs in various applications.

With this in mind, herein, we have designed and developed a new Zn(II)-coordination polymer, **TDPAT-Zn-CP**, utilizing the blue-emitting TDPAT linker to create a sensitive and selective fluorescent sensor for antibiotic detection. By exploiting the Lewis base characteristics of TDPAT, we anticipated enhanced selectivity of **TDPAT-Zn-CP** towards antibiotics through intermolecular hydrogen bonding interactions between the polymer and antibiotic analytes. Fluorescence titration studies confirmed this hypothesis by demonstrating that **TDPAT-Zn-CP** preferentially binds to sulfamethazine (SMZ) antibiotics, exhibiting exceptional sensitivity in detecting trace amounts of this antibiotic. The following sections provide the synthesis, characterization, and fluorescence-based sensing properties of **TDPAT-Zn-CP** towards antibiotics in aqueous medium.

2. Experimental

2.1. Materials

All reagents, starting materials, and solvents were purchased from Sigma-Aldrich (Bangalore, India) and used without further purification. Commercially available reagent-grade chemicals were utilized for the synthesis of TDPAT and **TDPAT-Zn-CP**. Spectroscopy-grade solvents from Merck were used as received. Cyanuric chloride, di-2-pyridylamine, toluene, and sodium hydroxide were also obtained from Sigma-Aldrich and used without additional purification. Reagent-grade antibiotic analytes for sensing experiments were sourced from the Tokyo Chemical Industry (Hyderabad, India). The organic linker TDPAT was synthesized following the procedure outlined in the literature [33].

2.2. Instrumentations

Powder X-ray diffraction (PXRD) analysis of **TDPAT-Zn-CP** was conducted using a Rigaku X-ray diffractometer with Cu-Kα radiation (λ = 1.5418 Å) over a 2θ range of 10° to 90°. Fourier transform infrared (FT-IR) spectra were recorded on a Shimadzu IR Tracer 100 equipped with an attenuated total reflectance (ATR) sampler, maintaining the sample at room temperature during the measurement. The morphology and surface characteristics of **TDPAT-Zn-CP** were examined using field emission scanning electron microscopy (FE-SEM) on a Carl Zeiss Gemini SEM 300 (ZEISS Microscopy, Oberkochen,

Germany). Before imaging, an aqueous solution of the synthesized polymer was drop-cast onto a sample stub, followed by gold coating and vacuum drying. Thermogravimetric analysis (TGA) was performed on a PerkinElmer STA 8000 analyzer (PerkinElmer, Thane, India) with a temperature scan rate of 10 °C/min from 30 °C to 800 °C under a nitrogen atmosphere. Dynamic light scattering (DLS) measurements were conducted on a Malvern Panalytical Zetasizer (Malvern Panalytical, Worcestershire, UK) at the PSG Institute of Advanced Studies in Coimbatore to assess the particle size distribution of **TDPAT-Zn-CP**. UV-visible absorption spectra were obtained using a Thermo Fisher Scientific absorption spectrometer (Thermo Fisher Scientific, Waltham, MA, USA), with baseline correction applied to all recorded values. Fluorescence titration experiments were carried out using a PerkinElmer FL-8500 fluorescence spectrophotometer (PerkinElmer, Thane, India), equipped with a 150 W Xenon arc lamp. The slit width was set to 10 nm, and the scan rate was 1200 nm/min, with all measurements conducted at room temperature. Data analysis and graphical representation were performed using Origin Pro 8.5 software.

2.3. Synthesis of **TDPAT-Zn-CP**

In a typical synthesis, 100 mg of the organic ligand TDPAT (0.17 mmol, 2 eq.) was dissolved in 20 mL of ethanol and sonicated to form a homogeneous solution. To this, 56 mg of zinc acetate dihydrate (0.26 mmol, 3 eq.) dissolved in 20 mL of H_2O was added dropwise and then stirred at room temperature to obtain a clear solution. The resulting mixture was then heated in an oil bath at 60 °C for 48 h. After completion of the reaction, the mixture was allowed to cool, and the resulting white precipitate was collected by filtration and washed with distilled water, followed by ethanol. The final product was washed with diethyl ether and dried at room temperature, resulting in a white powder of **TDPAT-Zn-CP** with an isolated yield of 52% (calculated based on TDPAT).

2.4. Fluorescence Sensing Studies

A stock solution of **TDPAT-Zn-CP** was prepared by dispersing 2 mg of the polymer in 10 mL of deionized water. The mixture was sonicated for 30 min and then allowed to age for 24 h, forming a stable colloidal suspension. Aqueous solutions of antibiotics were prepared at a concentration of 1 mM. For the fluorescence sensing experiments, 100 µL of the colloidal suspension of **TDPAT-Zn-CP** was diluted with 1900 µL of H_2O in a 3 mL cuvette. The fluorescence emission was recorded before and after the addition of antibiotic analytes. Fluorescence titration experiments were conducted by adding 10 µL aliquots of antibiotic solutions to the cuvette containing **TDPAT-Zn-CP**. The solution was excited at λ = 287 nm, and the emission was monitored between λ = 350 and 550 nm at room temperature. A slit width of 10 nm was maintained for all measurements. The fluorescence quenching efficiency was calculated using the following equation:

$$\text{Quenching efficiency} = (I_0 - I)/I_0 \times 100$$

where I_0 is the fluorescence intensity of **TDPAT-Zn-CP** in H_2O before the addition of the antibiotic, and I is the fluorescence intensity after the antibiotic was added. The relationship between the fluorescence intensity ratio (I_0/I) and antibiotic concentration [Q] was analyzed using the Stern–Volmer equation:

$$(I_0/I) = 1 + K_{SV}[Q]$$

Here, the slope of the linear plot corresponds to the Stern–Volmer quenching constant (K_{SV}). The limit of detection (LoD) was calculated using the formula:

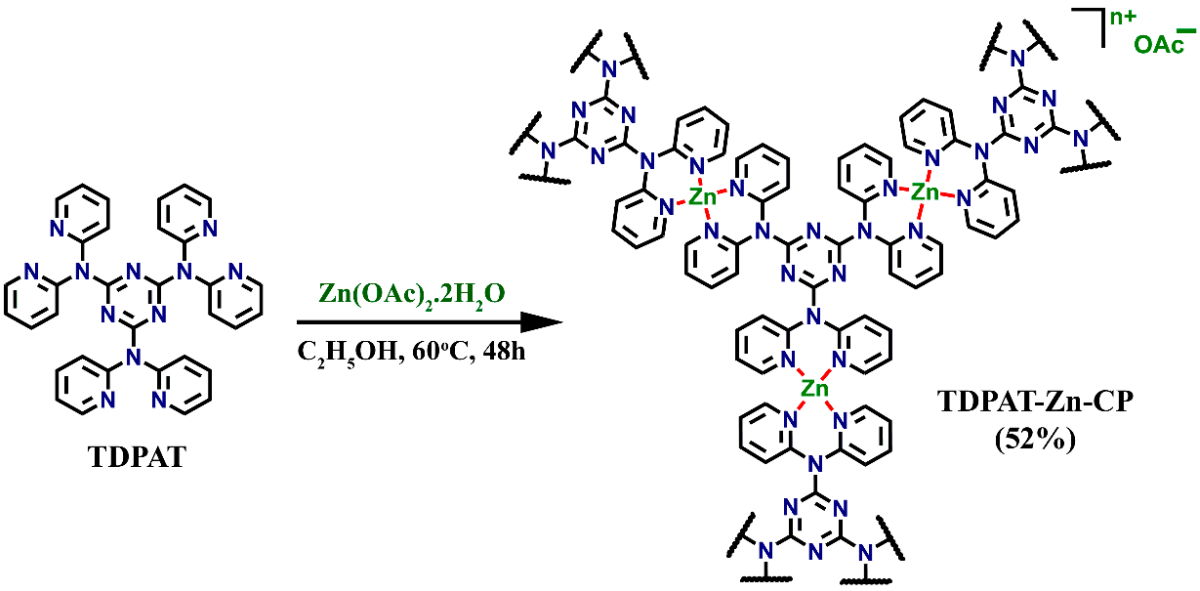
$$\text{Limit of detection (LoD)} = 3\sigma/\text{K}.$$

where σ is the standard deviation of the fluorescence intensity of **TDPAT-Zn-CP** in the absence of any analyte, and K is the slope of the linear calibration plot in which fluorescence intensity is recorded concerning the concentration of antibiotics in nM concentration.

3. Results and Discussion

3.1. Synthesis and Characterization of **TDPAT-Zn-CP**

The organic linker TDPAT was synthesized using a previously reported method, where cyanuric chloride was reacted with di-2-pyridylamine in the presence of toluene and sodium hydroxide under reflux conditions, resulting in a high yield of the TDPAT ligand. This ligand was then employed to synthesize the coordination polymer **TDPAT-Zn-CP** by stirring the solution of TDPAT (2.0 eq.) in ethanol with $Zn(OAc)_2{\cdot}2H_2O$ (3.0 eq.) in H_2O at 60 °C for 48 h, as depicted in Scheme 1. Mixing $Zn(OAc)_2{\cdot}2H_2O$ caused the initially clear TDPAT solution to form a white colloidal suspension, indicating the polymerization process. After cooling, the heavy precipitate formed was isolated by filtration, and the precipitate was washed with water, ethanol, and diethyl ether, resulting in a white powder of **TDPAT-Zn-CP** (in 52% yield).



Scheme 1. Schematic representation of the synthesis of Zn(II) coordination polymer **TDPAT-Zn-CP** from TDPAT.

TDPAT-Zn-CP was characterized using various spectroscopic and analytical techniques to ascertain its structural, thermal, and morphological properties. The infrared spectrum of **TDPAT-Zn-CP** displayed key vibrational bands indicative of the coordination environment and functional groups present in the polymer (Figure 1A). Specifically, the bands at ν = 1585 cm^{-1} and 1456 cm^{-1} were attributed to the asymmetrical and symmetrical stretching vibrations of the carboxylate (COO^-) counter anions. Two prominent bands at ν = 1535 and 1377 cm^{-1} correspond to the triazine ring, which confirms the presence of triazine moieties in the isolated polymer. The Zn−N coordination bond formation was indicated by a sharp band observed at ν = 496 cm^{-1} corresponding to the Zn−N stretching vibration. The C=O stretching vibration of the COO^- anion was observed as a weak band

around ν = 1751 cm^{-1}, which could be attributed to the effective delocalization of the negative charge across the COO^- anion.

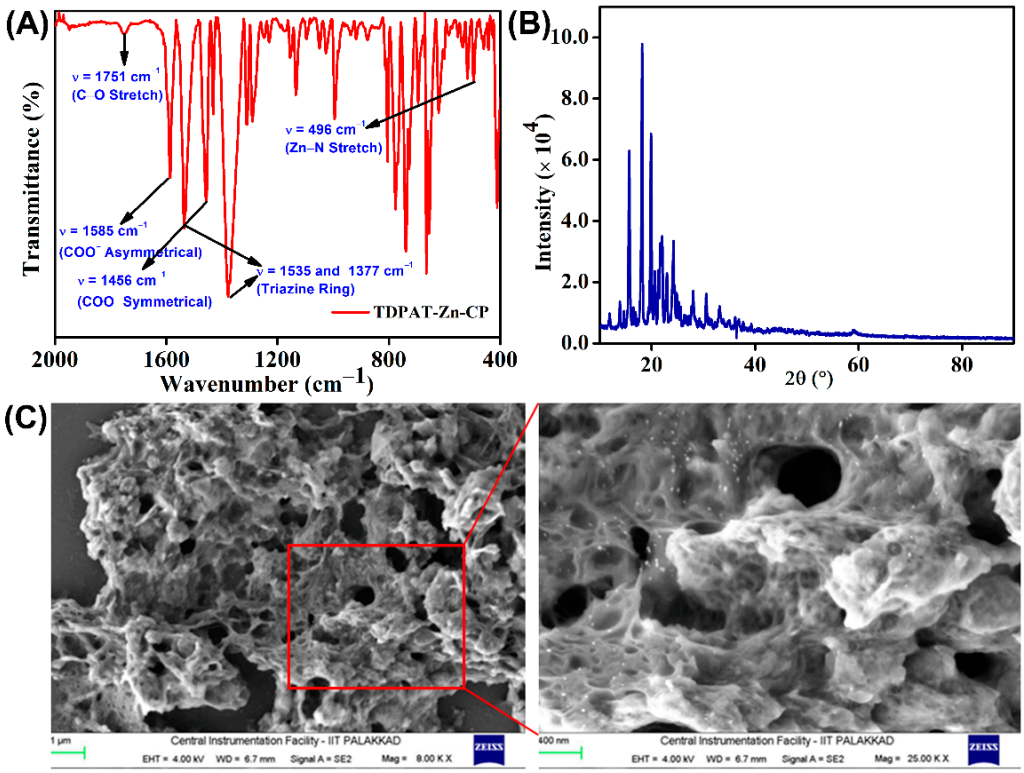


Figure 1. (**A**) FT-IR spectrum, (**B**) powder X-ray diffraction pattern, and (**C**) SEM images at different magnifications of **TDPAT-Zn-CP**.

Furthermore, the crystallinity of the **TDPAT-Zn-CP** was evaluated through powder XRD analysis, where sharp diffraction peaks were observed, suggesting a well-defined crystalline structure of the coordination polymer (Figure 1B). This is a hallmark of the ordered arrangement of the polymer chains and metal centers. DLS measurements, conducted in an aqueous medium, determined the average particle size of **TDPAT-Zn-CP** to be approximately nanometer (nm) scale, indicating that the polymer exists as a polydispersed nanoscale material (see Figure S2, ESI). Additionally, the TGA curve revealed that the polymer remained thermally stable up to 300 °C, with an initial weight loss of 6.5% observed between 300 °C and 400 °C, attributed to removing volatile components trapped within the polymeric networks. Approximately 10% of the polymer mass was retained at 600 °C (see Figure S1, ESI), demonstrating its relative thermal stability. Scanning electron microscopy (SEM) imaging was performed to examine the surface morphology, and the results revealed a sponge-like structure with a nanoporous texture, as depicted in Figure 1C. This unique morphology suggests that the **TDPAT-Zn-CP** has a high surface area and porosity, which could be advantageous for applications in adsorption or catalysis. Further, the energy-dispersive X-ray spectroscopy (EDX) confirmed the presence of Zn, N, C, and O elements in the isolated coordination polymer (Figure S3, ESI).

3.2. Antibiotics Sensing Properties of **TDPAT-Zn-CP**

TDPAT-Zn-CP has significant potential for antibiotic detection due to its electron-rich nature and the presence of Lewis base functional groups, which can facilitate donor–acceptor interactions with electron-deficient antibiotics, thereby enabling fluorescence-based sensing. The UV-visible absorption spectrum of **TDPAT-Zn-CP** dispersed in an aqueous solution displayed a broad, intense peak centered at λ = 285 nm ascribed to π–π*

transitions (see Figure S4A, ESI). The fluorescence emission spectrum of **TDPAT-Zn-CP** recorded in an aqueous solution exhibited a broad emission band centered at λ = 452 nm (see Figure S4B, ESI). Given the strong fluorescence emission, the antibiotic sensing properties of **TDPAT-Zn-CP** were studied by measuring the changes in emission intensity before and after the addition of various antibiotics in aqueous media.

In this study, a group of ecologically relevant antibiotics, including Chloramphenicol (CRP), Nitrofurazone (NFZ), Nitrofurantoin (NFT), Furazolidone (FZD), Sulfadiazine (SDZ), and Sulfamethazine (SMZ), were chosen to evaluate the sensing capabilities of **TDPAT-Zn-CP** (see Figure 2 for the structure). Stock solutions of 1 mM concentration of each antibiotic were prepared in Milli-Q water to ensure consistent test conditions. As shown in Figure 3A,B, the extent of fluorescence quenching varied significantly for different antibiotics. Among the tested antibiotics, SMZ exhibited a prominent fluorescence quenching, suggesting its strong interactions with **TDPAT-Zn-CP**. The addition of other antibiotics showed moderate to poor fluorescence quenching, indicating their weaker interactions with the polymer.

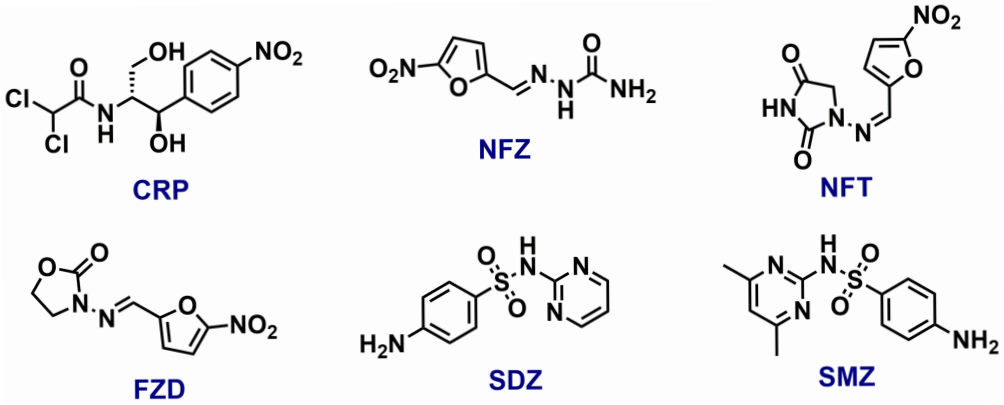


Figure 2. The structure of different antibiotics used in this study.

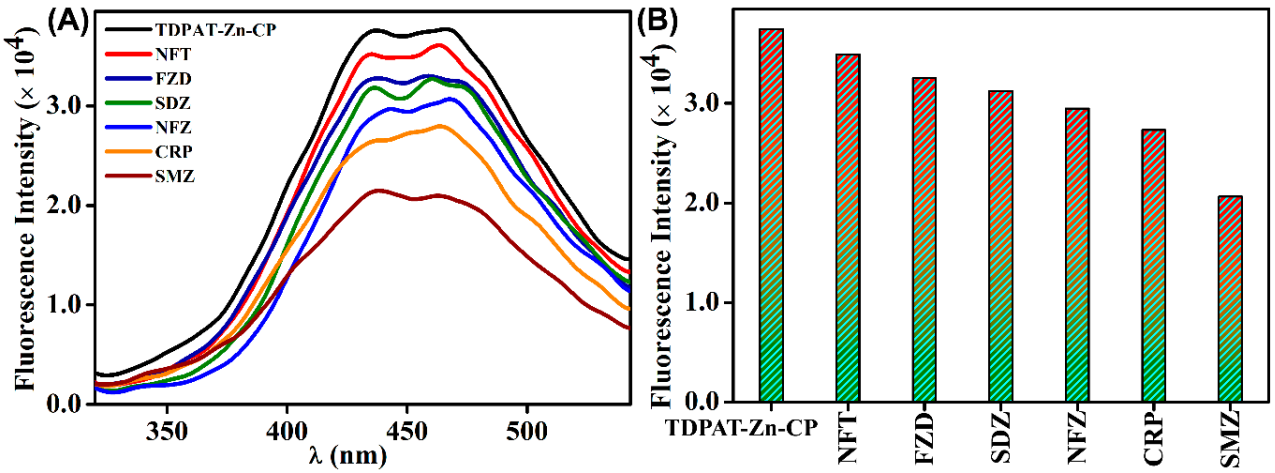


Figure 3. (**A**) The extent of fluorescence quenching observed for **TDPAT-Zn-CP** in water after adding different antibiotics and (**B**) their corresponding bar diagram.

Furthermore, a fluorescence titration experiment was performed to understand the sensing capability of **TDPAT-Zn-CP** towards SMZ. As shown in Figure 4A, the initial emission maxima at λ = 452 nm of **TDPAT-Zn-CP** were significantly quenched upon the gradual addition of SMZ (0.0 → 107 μM) antibiotics. The quenching efficiency of **TDPAT-Zn-CP** towards SMZ was calculated as 45%, further confirming the preferential binding affinity between the sensor and SMZ. To quantitatively evaluate the interaction,

a linear Stern–Volmer plot was obtained from the fluorescence intensity versus the antibiotic concentration, and the slope of this linear plot was used to calculate the K_{SV}, which was determined to be 1.68×10^4 M^{-1}. The high value of K_{SV} indicates the strong binding affinity between the sensor and antibiotics. For comparative analysis, K_{SV} for other antibiotics was also determined and summarized in Table 1. The quenching constants for these antibiotics, including NFZ, CRP, NFT, FZD, and SDZ, exhibited a range of values, which were in line with those reported for other Zn(II) coordination polymer-based sensors designed for antibiotic fluorescence sensing [24]. These results highlight the selective and high-affinity interaction of **TDPAT-Zn-CP** with specific antibiotics, particularly SMZ, which showed the highest quenching efficiency.

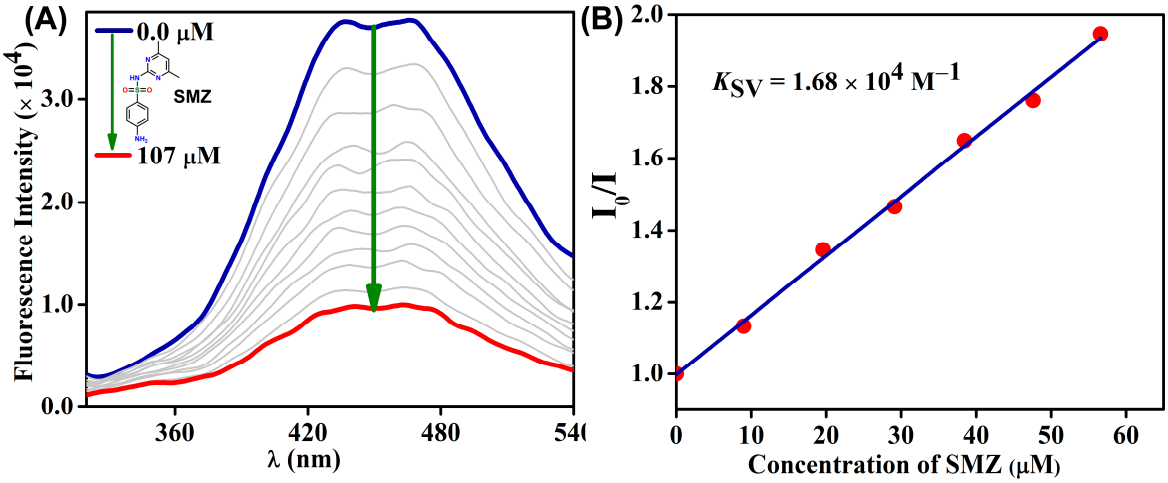


Figure 4. (**A**) The changes in fluorescence emission intensity of **TDPAT-Zn-CP** upon increased addition of SMZ (in μM) in water and (**B**) its corresponding Stern–Volmer Plot.

Table 1. The K_{SV} value for different antibiotics was calculated from their corresponding fluorescence titration profile.

Antibiotics	K_{SV} (M^{-1})
SMZ	1.68×10^4
NFT	3.8×10^3
CRP	6.5×10^3
NFZ	4.8×10^3
FZD	4.0×10^3
SDZ	4.2×10^3

A UV-visible absorption titration experiment was conducted to investigate further the interaction between **TDPAT-Zn-CP** and SMZ. As shown in Figure 5A, the addition of increasing concentrations of SMZ (ranging from 0.0 to 56 μM) resulted in the disappearance of the band at λ = 285 nm and the gradual appearance of two new bands at λ = 263 and 239 nm, indicating the strong interactions and further confirms the formation of a ground-state charge transfer (CT) complex between SMZ and **TDPAT-Zn-CP**. This observation supports the notion that the binding between the polymer and the antibiotic occurs in the ground state, consistent with a ground-state quenching mechanism. To corroborate this mechanism, time-dependent fluorescence lifetime measurements were performed (Figure 5B). The fluorescence lifetime of **TDPAT-Zn-CP** (τ = 0.71 ns) remained relatively unchanged with the addition of SMZ (0 → 240 μM), with only a slight increase of approximately 0.07 ns. This

minimal change in lifetime further confirms the static quenching effect. Interestingly, the fluorescence titration studies also demonstrated the high sensitivity of **TDPAT-Zn-CP** for SMZ detection, which was detectable even at nanomolar concentrations (Figure S5, ESI). A limit of detection (LoD) value of 4.95 ppb was determined, which is significantly lower than many other fluorescence-based sensors for antibiotic detection, indicating the high sensitivity and suitability of **TDPAT-Zn-CP** for environmental and clinical applications.

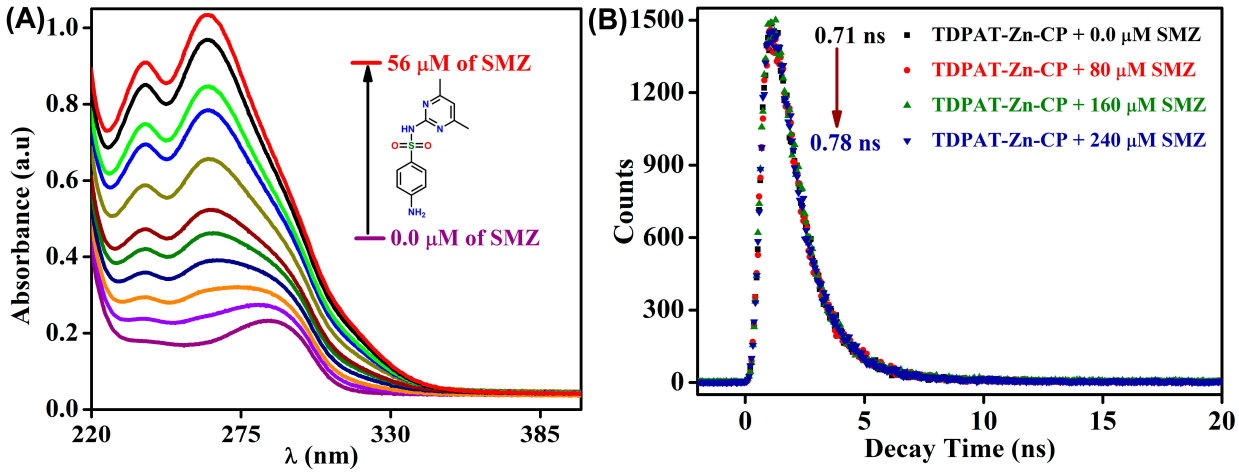


Figure 5. (**A**) The changes in absorption spectra of **TDPAT-Zn-CP** upon increased addition of SMZ (0.0 → 56 μM) in water and (**B**) time-dependent fluorescence lifetime measurements.

4. Conclusions

In conclusion, we have successfully developed a new nitrogen-rich luminescent Zn(II) coordination polymer, **TDPAT-Zn-CP**, incorporating the 2,4,6-tris(di-2-pyridyl amino)-1,3,5-triazine structural motif. Comprehensive characterization through spectroscopy and microscopy confirmed its crystalline structure, sponge-like morphology, and remarkable thermal stability. **TDPAT-Zn-CP** exhibited differential fluorescence sensing towards various antibiotics with a preferential affinity for SMZ, demonstrating substantial fluorescence quenching with high sensitivity. Moreover, ongoing investigations are focused on enhancing the TDPAT-based zinc coordination polymer system as a molecular sieve and adsorbent, with promising applications in the removal of organic emerging pollutants from water. Overall, this work highlights the versatility and potential of **TDPAT-Zn-CP** in environmental sensing and water remediation, opening avenues for future advancements in sustainable water quality management.

Supplementary Materials: The following supporting information can be downloaded at: https://www.mdpi.com/article/10.3390/chemistry7040108/s1, Figure S1. Thermogravimetric analysis of as-synthesized **TDPAT-Zn-CP**; Figure S2. The size distribution of **TDPAT-Zn-CP** particles in aqueous medium was obtained using Dynamic Light Scattering measurement; Figure S3. Energy dispersive spectroscopy indicating the elemental composition of **TDPAT-Zn-CP**; Figure S4. (A) UV-visible absorption and (B) fluorescence emission spectra for **TDPAT-Zn-CP** recorded in water at room temperature; Figure S5. The observed changes in emission intensity for **TDPAT-Zn-CP** upon the gradual addition of SMZ at the nanomolar level.

Author Contributions: Investigation, S.P.B. and M.K.N.; writing—original draft preparation, S.P.B., M.K.N., B.M. and S.S.; writing—review and editing, M.K.N. and S.S.; supervision, S.S.; project administration, S.S.; funding acquisition, S.S. All authors have read and agreed to the published version of the manuscript.

Funding: Indian Institute of Technology Palakkad (ERG research grant 2023-168-CHY-SHS-ERG-SP to S.S.) and Science and Engineering Research Board, India (EMEQ research grant EEQ/2023/000386 to S.S.).

Data Availability Statement: The raw data supporting the conclusions of this article will be made available by the authors upon request.

Acknowledgments: The authors thank the Central Instrumentation Facility (CIF) at IIT Palakkad for its research facilities.

Conflicts of Interest: The authors declare no conflicts of interest.

References

1. Mesak, L.R.; Miao, V.; Davies, J. Effects of Subinhibitory Concentrations of Antibiotics on SOS and DNA Repair Gene Expression in Staphylococcus aureus. *Antimicrob. Agents Chemother.* **2008**, *52*, 3394–3397. [CrossRef]
2. Zhang, Q.-Q.; Ying, G.-G.; Pan, C.-G.; Liu, Y.-S.; Zhao, J.-L. Comprehensive Evaluation of Antibiotics Emission and Fate in the River Basins of China: Source Analysis, Multimedia Modeling, and Linkage to Bacterial Resistance. *Environ. Sci. Technol.* **2015**, *49*, 6772–6782. [CrossRef]
3. Mungroo, N.; Neethirajan, S. Biosensors for the Detection of Antibiotics in Poultry Industry—A Review. *Biosensors* **2014**, *4*, 472–493. [CrossRef]
4. Klein, E.Y.; Van Boeckel, T.P.; Martinez, E.M.; Pant, S.; Gandra, S.; Levin, S.A.; Goossens, H.; Laxminarayan, R. Global Increase and Geographic Convergence in Antibiotic Consumption Between 2000 and 2015. *Proc. Natl. Acad. Sci. USA* **2018**, *115*, E3463–E3470. [CrossRef] [PubMed]
5. Huang, D.; Wang, X.; Zhang, C.; Zeng, G.; Peng, Z.; Zhou, J.; Cheng, M.; Wang, R.; Hu, Z. Sorptive Removal of Ionizable Antibiotic Sulfamethazine from Aqueous Solution by Graphene Oxide-Coated Biochar Nanocomposites: Influencing Factors and Mechanism. *Chemosphere* **2017**, *186*, 414–421. [CrossRef] [PubMed]
6. Zhang, J.; Sui, Q.; Tong, J.; Zhong, H.; Wang, Y.; Chen, M.; Wei, Y. Soil Types Influence the Fate of Antibiotic-Resistant Bacteria and Antibiotic Resistance Genes Following the Land Application of Sludge Composts. *Environ. Int.* **2018**, *118*, 34–43. [CrossRef] [PubMed]
7. Hirsch, R.; Ternes, T.; Haberer, K.; Kratz, K.-L. Occurrence of Antibiotics in the Aquatic Environment. *Sci. Total Environ.* **1999**, *225*, 109–118. [CrossRef]
8. Morrison, L.; Zembower, T.R. Antimicrobial Resistance. *Gastrointest. Endosc. Clin. N. Am.* **2020**, *30*, 619–635. [CrossRef]
9. Davies, J. What are Antibiotics? Archaic Functions for Modern Activities. *Mol. Microbiol.* **1990**, *4*, 1227–1232. [CrossRef]
10. Raja Lakshmi, P.; Nanjan, P.; Kannan, S.; Shanmugaraju, S. Recent Advances in Luminescent Metal–Organic Frameworks (LMOFs) based Fluorescent Sensors for Antibiotics. *Coord. Chem. Rev.* **2021**, *435*, 213793. [CrossRef]
11. Liu, Y.; Wang, J. Degradation of Sulfamethazine by Gamma Irradiation in the Presence of Hydrogen Peroxide. *J. Hazard. Mater.* **2013**, *250–251*, 99–105. [CrossRef]
12. Li, Y.-T.; Qu, L.-L.; Li, D.-W.; Song, Q.-X.; Fathi, F.; Long, Y.-T. Rapid and Sensitive In-Situ Detection of Polar Antibiotics in Water Using a Disposable Ag–Graphene Sensor based on Electrophoretic Preconcentration and Surface-Enhanced Raman Spectroscopy. *Biosens. Bioelectron.* **2013**, *43*, 94–100. [CrossRef] [PubMed]
13. Wang, Z.; Xing, K.; Ding, N.; Wang, S.; Zhang, G.; Lai, W. Lateral Flow Immunoassay based on Dual Spectral-Overlapped Fluorescence Quenching of Polydopamine Nanospheres for Sensitive Detection of Sulfamethazine. *J. Hazard. Mater.* **2022**, *423*, 127204. [CrossRef]
14. Xu, S.; Shi, J.-J.; Ding, B.; Liu, Z.-Y.; Wang, X.-G.; Zhao, X.-J.; Yang, E.-C. A Heterometallic Sodium(I)–Europium(III)-Organic Layer Exhibiting Dual-Responsive Luminescent Sensing for Nitrofuran Antibiotics, $Cr_2O_7^{2-}$ and MnO_4^- anions. *Dalton Trans.* **2019**, *48*, 1823–1834. [CrossRef] [PubMed]
15. Aguilera-Luiz, M.M.; Vidal, J.L.M.; Romero-González, R.; Frenich, A.G. Multi-Residue Determination of Veterinary Drugs in Milk by Ultra-High-Pressure Liquid Chromatography–Tandem Mass Spectrometry. *J. Chromatogr. A* **2008**, *1205*, 10–16. [CrossRef] [PubMed]
16. Li, D.; Yang, M.; Hu, J.; Zhang, Y.; Chang, H.; Jin, F. Determination of Penicillin G and Its Degradation Products in a Penicillin Production Wastewater Treatment Plant and the Receiving River. *Water Res.* **2008**, *42*, 307–317. [CrossRef]
17. Paul, T.; Miller, P.L.; Strathmann, T.J. Visible-Light-Mediated TiO_2 Photocatalysis of Fluoroquinolone Antibacterial Agents. *Environ. Sci. Technol.* **2007**, *41*, 4720–4727. [CrossRef]
18. Cinquina, A.L.; Longo, F.; Anastasi, G.; Giannetti, L.; Cozzani, R. Validation of A High-Performance Liquid Chromatography Method for the Determination of Oxytetracycline, Tetracycline, Chlortetracycline and Doxycycline in Bovine Milk and Muscle. *J. Chromatogr. A* **2003**, *987*, 227–233. [CrossRef]
19. González, O.; Sans, C.; Esplugas, S. Sulfamethoxazole Abatement by Photo-Fenton. *J. Hazard. Mater.* **2007**, *146*, 459–464. [CrossRef]
20. Shanmugaraju, S.; Mukherjee, P.S. π-Electron Rich Small Molecule Sensors for the Recognition of Nitroaromatics. *Chem. Commun.* **2015**, *51*, 16014–16032. [CrossRef]

21. Zhao, J.; Wang, Y.-N.; Dong, W.-W.; Wu, Y.-P.; Li, D.-S.; Zhang, Q.-C. A Robust Luminescent Tb(III)-MOF with Lewis Basic Pyridyl Sites for the Highly Sensitive Detection of Metal Ions and Small Molecules. *Inorg. Chem.* **2016**, *55*, 3265–3271. [CrossRef]
22. Germain, M.E.; Knapp, M.J. Optical Explosives Detection: From Color Changes to Fluorescence Turn-on. *Chem. Soc. Rev.* **2009**, *38*, 2543. [CrossRef] [PubMed]
23. Nagarkar, S.S.; Desai, A.V.; Ghosh, S.K. A Fluorescent Metal-Organic Framework for Highly Selective Detection of Nitro Explosives in the Aqueous Phase. *Chem Commun.* **2014**, *50*, 8915–8918. [CrossRef] [PubMed]
24. Zhu, X.-D.; Zhang, K.; Wang, Y.; Long, W.-W.; Sa, R.-J.; Liu, T.-F.; Lü, J. Fluorescent Metal-Organic Framework (MOF) as a Highly Sensitive and Quickly Responsive Chemical Sensor for the Detection of Antibiotics in Simulated Wastewater. *Inorg. Chem.* **2018**, *57*, 1060–1065. [CrossRef] [PubMed]
25. Kreno, L.E.; Leong, K.; Farha, O.K.; Allendorf, M.; Van Duyne, R.P.; Hupp, J.T. Metal-Organic Framework Materials as Chemical Sensors. *Chem. Rev.* **2012**, *112*, 1105–1125. [CrossRef]
26. Lin, X.; Hong, Y.; Zhang, C.; Huang, R.; Wang, C.; Lin, W. Pre-Concentration and Energy Transfer Enable the Efficient Luminescence Sensing of Transition Metal Ions by Metal–Organic Frameworks. *Chem. Commun.* **2015**, *51*, 16996–16999. [CrossRef]
27. Li, B.; Wen, H.-M.; Wang, H.; Wu, H.; Tyagi, M.; Yildirim, T.; Zhou, W.; Chen, B. A Porous Metal–Organic Framework with Dynamic Pyrimidine Groups Exhibiting Record High Methane Storage Working Capacity. *J. Am. Chem. Soc.* **2014**, *136*, 6207–6210. [CrossRef]
28. Van De Voorde, B.; Bueken, B.; Denayer, J.; De Vos, D. Adsorptive Separation on Metal–Organic Frameworks in the Liquid Phase. *Chem Soc Rev.* **2014**, *43*, 5766–5788. [CrossRef]
29. Mohammadikish, M.; Ghanbari, S. Preparation of Monodispersed Metal-based Infinite Coordination Polymer Nanostructures and Their Good Capability for Metal Oxide Preparation. *J. Solid State Chem.* **2018**, *264*, 86–90. [CrossRef]
30. Patel, P.; Noushija, M.K.; Shanmugaraju, S. Differential Fluorescent Chemosensing of Antibiotics Using a Luminescent Zn(II) Coordination Polymer Based on a 4-Amino-1,8-naphthalimide Tröger's Base Fluorophore. *Chemistry* **2024**, *6*, 237–248. [CrossRef]
31. Shanmugaraju, S.; Dabadie, C.; Byrne, K.; Savyasachi, A.J.; Umadevi, D.; Schmitt, W.; Kitchen, J.A.; Gunnlaugsson, T. A Supramolecular Tröger's base Derived Coordination Zinc Polymer for Fluorescent Sensing of Phenolic-Nitroaromatic Explosives in Water. *Chem. Sci.* **2017**, *8*, 1535–1546. [CrossRef] [PubMed]
32. Rasin, P.; Ashwathi, A.V.; Basheer, S.M.; Haribabu, J.; Santibanez, J.F.; Garrote, C.A.; Arulraj, A.; Mangalaraja, R.V. Exposure to Cadmium and Its Impacts on Human Health: A Short Review. *J. Hazard. Mater. Adv.* **2025**, *17*, 100608. [CrossRef]
33. Pang, J.; Tao, Y.; Freiberg, S.; Yang, X.-P.; D'Iorio, M.; Wang, S. Syntheses, Structures, and Electroluminescence of New Blue Luminescent Star-Shaped Compounds based on 1,3,5-triazine and 1,3,5-trisubstituted benzene. *J. Mater. Chem.* **2002**, *12*, 206–212. [CrossRef]

Disclaimer/Publisher's Note: The statements, opinions and data contained in all publications are solely those of the individual author(s) and contributor(s) and not of MDPI and/or the editor(s). MDPI and/or the editor(s) disclaim responsibility for any injury to people or property resulting from any ideas, methods, instructions or products referred to in the content.